By Christophe Turpin, Benoît Morin, Eric Bru,
Olivier Rallières, Xavier Roboam, Bruno Sareni,
Marcos Garcia Arregui, and Nicolas Roux

Power for Aircraft Emergencies

A hybrid proton-exchange membrane H_2/O_2 fuel cell and ultracapacitor system.

IN THE CONTEXT OF AVIATION, THIS article looks at replacing a ram air turbine (RAT) with a hybrid proton-exchange membrane (PEM) hydrogen/oxygen (H_2/O_2) fuel cell and ultracapacitor system, starting from a theoretical perspective. The structure we propose has two static power converters: one associated with fuel cells and the other with ultracapacitors. The energy management principle presented (frequency sharing) enables two types of control. First, the converter associated with the fuel cell manages the voltage of the dc bus, and then the converter associated with the ultracapacitors controls the high-frequency currents. Second, the voltage of the dc bus is oppositely controlled by the ultracapacitor converter.

An experimental validation (at a reduced ratio scale of 1:10) allows for an analysis of the proposed principles. The experiment is conducted in two stages. In the initial validation, a fuel cell physical emulator is used as the main source, before introducing an actual fuel cell.

Fuel Cells and Aircraft

In the context of the More Electric Aircraft (Weimer 1993), one of the concepts supported by the European More Open Electrical Technologies project, the electrical power requirements of an aircraft are set to increase (Roboam et al. 2012) thanks to recent advances in power electronics (Rosero et al. 2007). An aircraft may be subject to various failures, in particular to the total loss of the engines or electrical power. These failures must remain acceptable (Mehdi and Woods 1989). For most large aircraft, a backup system composed of a RAT is used to generate emergency power (Bolognesi 2009). As new and future flight control actuators are electrical (Van Den Bossche 2003), the load profile supplied by this backup system is very intermittent (Figure 1). As the increase in electrical power demand is becoming very restrictive for the aircraft structure, which must include an increasingly large RAT, researchers have been looking at replacing this turbine with a fuel cell (Garcia-Arregui 2007). In addition, a fuel cell system has other advantages compared to the current RAT system's properties (Wörner 2009): it operates independently of the aircraft's speed and altitude; it can be stopped at any time if the main engines are recovered, while the RAT cannot be retracted once it has been extended; and it may reduce maintenance. Motapon et al. have also recently conducted and presented research in Canada with experimental tests on replacing the RAT with a hybrid fuel cell.

The fuel cell indirectly [via reduction–oxidation reaction (redox)] makes H_2 react with O_2 (Pera et al. 2013). There are several possible strategies for supplying the gases (Garcia-Arregui 2007). H_2 may be produced on board by reforming kerosene (Lenz and Aicher 2005, Ibarreta and Sung 2006), or embedded in a compressed form. O_2 may be taken from the ambient air using a compressor or carried in a compressed form. All scenarios were examined and assessed by Garcia-Arregui, and the most relevant solution for the emergency power application would be carrying both gases in a compressed form, which would eliminate the complex stage of reforming the kerosene and ensuring the quantity and/or quality of the air in the event of an emergency. This H_2/O_2 solution is studied and experimentally validated in this article.

Research on fuel cell applications in aviation goes beyond the mere use in emergency power units (Curtin 2010). A fuel cell could replace the gas turbine that currently performs the auxiliary power unit (APU) function, which essentially supplies the aircraft with power when it is on the ground. This would reduce aircraft noise and gas emissions on the ground. A hybrid fuel cell/battery system has been proposed to perform this function (Eid et al. 2010). Looking even further into the future, the hybridization of a high-temperature fuel cell and a turbine for this APU has been studied (Rajashekara et al. 2008). In the Elektrische Basissysteme in einem CFK Rumpf: Architektur und Auslegung project (2007–2009, funded by the Federal Ministry of Economics and Technology/Airbus, EYI-058/07) in Germany, researchers are studying various applications based on fuel cells (Wörner 2009): the emergency power unit, multifunctional fuel cell system (power, water, and inerting), and green taxiing on the ground. Incorporating fuel cells in aviation would seem to require multifunctional technology to compete with the other current highly integrated technologies.

Given the intermittent character of the emergency profile to be achieved as displayed in Figure 1, it is useful to associate a source with high specific power with the main power source to avoid oversizing (Turpin et al. 2012). Therefore, the current RAT has already been the subject of optimization studies (to reduce its size and weight) by associating it with ultracapacitors (Roboam et al. 2011, Rafal et al. 2010) based on the duration of the intermittent loads to be satisfied (high power peaks but with relatively low energy). For a fuel cell emergency power unit, there is also the issue of not oversizing the fuel cell (Jiang and Dougal 2006). However, there are other reasons to justify this hybridization, such as in Martínez et al., or Bizon et al. for vehicles, e.g., for H_2/air operation, it can also be used to compensate for the dynamics of the air compression (Zhan et al. 2008).

The work in this article is in line with previous theoretical work conducted in the context of the European CELINA—Fuel Cell Application in a New Configured Aircraft—project. Several electrical architectures have been
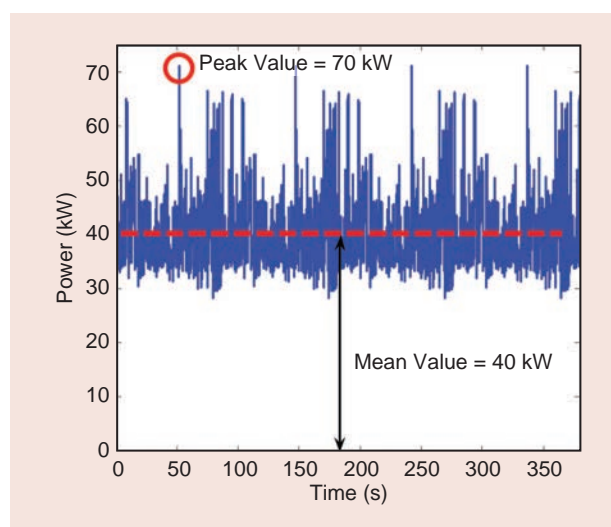
Figure 1. A typical load profile for the sizing of an emergency power system (approach phase).

studied (Garcia-Arregui 2007, Morin et al. 2014) for associating fuel cells with ultracapacitors. Here, the focus is on the architecture that uses two dc–dc converters: one for the fuel cell and the other for the ultracapacitor.

Description of the Hybrid System

Various loads used in an emergency may be considered constant. This is because the electronic equipment (computers) and anti-icing items absorb power that is constant over time for the duration of the emergency mission. Other equipment, such as fuel pumps, radio equipment, and lights, absorb constant power when used. However, some loads are very variable, in particular the flight control actuators, which require power that fluctuates substantially depending on the flight conditions and practically throughout the whole mission.

During the ground approach phase, the aircraft's speed is reduced, which means that a significant deflection of the flight control surfaces is required to direct the aircraft. This results in considerable power consumption. In addition, prior to landing, several maneuvers are performed by the pilot to adjust the position of the aircraft with respect to the target. The flight mission we selected (see Figure 1) is the low-speed ground approach phase of an aircraft flying in a turbulent environment with maneuvers controlled by the pilot. We defined this as the main mission for sizing our study (Garcia-Arregui 2007), i.e., highly variable power consumption that reaches the highest consumption peaks.

This mission profile has a mean power of 40 kW and consumption peaks reaching 70 kW, i.e., a 30-kW difference between the mean power to be supplied and the maximum sizing power for the system. An oversizing rate (OVSR) can be defined as follows:

$$OVSR = \frac{\max(\text{Power}) - \text{mean}(\text{Power})}{\max(\text{Power})}$$
$$= \frac{70e3 - 40e3}{70e3} = 0.42. \qquad (1)$$

An OVSR close to zero means that power consumption does not vary, while an OVSR close to one means that the sizing power is used only occasionally. In addition, generally speaking, a fuel cell requires fluidic auxiliaries with a slow dynamic response, whereas in an emergency mission, the required power must be available instantly. As a result, hybridization appears to be necessary in this case.

The new avionics standard that seems to be appearing in terms of the voltage level is a dc bus voltage of +270 Vdc/0 Vdc/–270 Vdc (Eid et al. 2010, Ravel 2009). The ultracapacitor is a good candidate for hybridization due to its qualities: high specific power, easy management of the state of charge, long lifetime and life cycles, and enough storable/returnable energy for our mission profile (Roboam et al. 2011, Langlois 2006, Maxwell Technologies Inc.).

Several solutions are possible for associating a fuel cell with ultracapacitors, as proposed by Garcia-Arregui. We take various criteria into account to classify the solutions: weight, gas consumption, stability of the dc bus, ease of use, fuel cell load current, filtering capacity of the ultracapacitors, and system reliability. According to Garcia-Arregui, the solution that offers the best compromise for our specifications is the one that uses two static converters: one for the fuel cell and the other for the ultracapacitors (Figure 2). This solution has the best bus stability and filtering capacity as well as middling weight and gas consumption, but its use and reliability are yet to be proven as the architecture puts a lot of strain on the power electronics.

We used several criteria to initially size the solution. The issue was to determine the optimal number of cells to be connected in series to create the fuel cell and their surface area. For example, it is possible to oversize the cell surface to reduce gas consumption. Weight is therefore saved for storing gas, but the fuel cell is made heavier so a compromise must be reached. An important criterion in sizing the power electronics is the minimum voltage of the fuel cell. At equivalent power, the lower the cell voltage, the higher the current flowing through the semiconductors.

As for the stored energy, it is important to ascertain its capacity and its minimum reference voltage, allowing for a discharge of less than
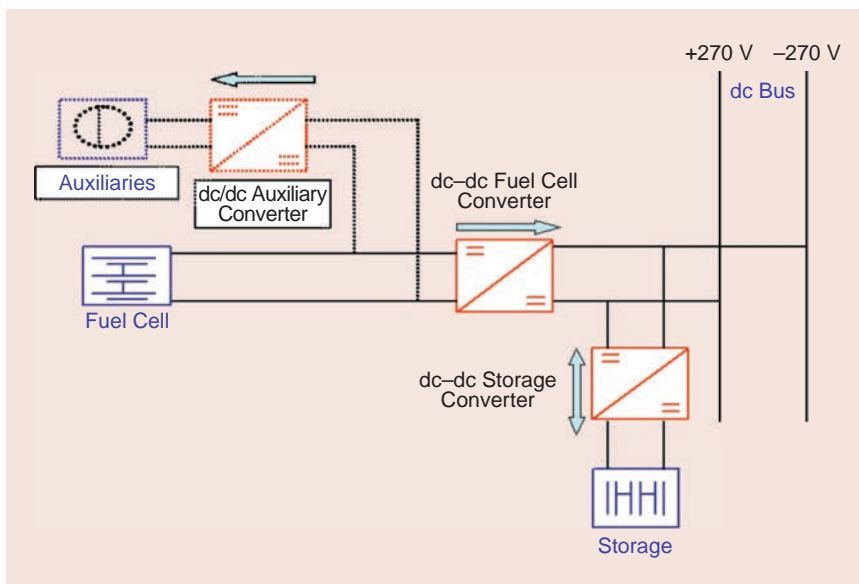
Figure 2. A solution using two dc–dc converters for the hybridization of a fuel cell and ultracapacitors.

50% of its voltage (i.e., 75% of its state of charge). The maximum voltage of the stored energy is used to determine the number of elements to be connected in series. Its capacity indicates how many branches of these elements are to be connected in parallel, with the elements being selected from ultracapacitor manufacturers' catalogues.

Table 1 contains an example of sizing, with an arbitrary choice of criteria to set some general figures. Subsequently, the following criteria remain variable to optimize the weight of the overall system and its gas consumption:

- fuel cell minimal voltage (V) = 100
- ultracapacitor maximal voltage (V) = 80
- ultracapacitor maximal discharge (%) = 50
- cutoff frequency (Hz) = 0.05
- fuel cell maximal current density (A/cm^2) = 0.5
- switching frequency (Hz) = 20,000
- number of parallel converter branches = four.

Theoretical Energy Management for the Studied Hybrid System

Frequency Sharing Principle

Hybridization in terms of power is defined as the association of various complementary sources. In our case, this association is achieved with a source of high specific energy (the fuel cell), which poorly withstands rapid variations in power (Schindele et al. 2005, Thounthong and Sethakul 2007), and a source of high specific power (ultracapacitors), which can only supply or absorb the mean power of zero (excluding losses). The idea of this power hybridization is to assign low variations in power to the fuel cell and zero mean power to the ultracapacitors. Several methods are available for this, including the distribution of frequency powers band and slope limitation. The method chosen for this study is power frequency sharing (Chapoulie and Astier 1998, Garcia-Arregui 2007) and is shown in Figure 3.

The desired filtering frequency will play a significant role in sizing the solution because, for a specific stored energy capacity, a lower frequency will cause the energy level of the ultracapacitors to fluctuate more. In other words, given the ultracapacitors' limitations (the maximum voltage level not to be exceeded and the minimum power reserve to be retained), at a given filtering frequency, a minimum stored energy capacity must be used for the system to be able to operate. In our case, this filtering frequency enabled us to size the stored energy capacity and its reference voltage. This frequency was recommended by a fuel cell manufacturer as the fastest frequency enabling the auxiliaries to correctly control the gas supply (the pressure and flow rate), despite the variations in fuel cell consumption.

An example of power frequency sharing is simulated in Figure 4. The presented case is an ideal scenario, taking into account neither the losses in the components nor the
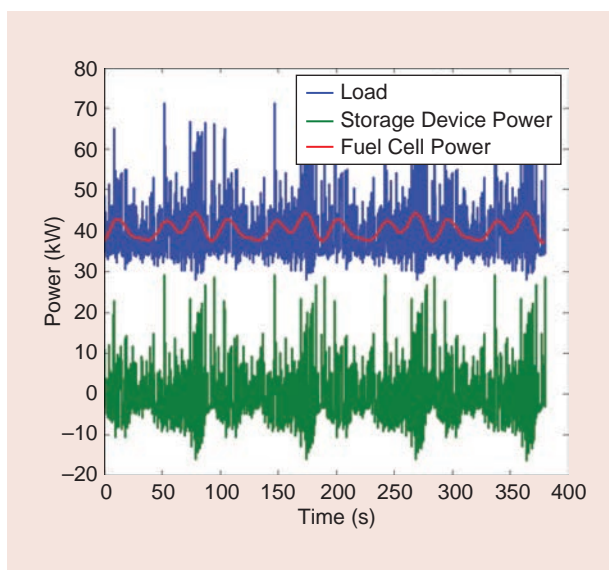
TABLE 1. An example of ideal hybrid system sizing (with no losses).

Fuel Cell Surface (cm^2)	Fuel Cell Number	C (F)	V_0 (V)
627.2	154	9.83	61.16

C: equivalent capacitance of ultracapacitors; V_0: Initial ultracapacitor voltage.
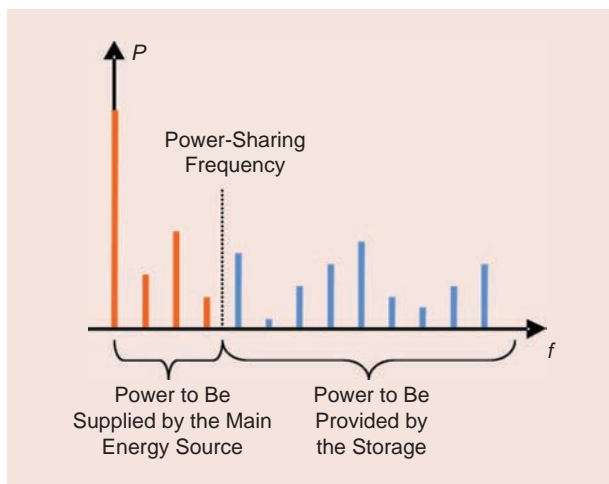
Figure 3. The principle of hybridization by frequency filtering, illustrated in a power–frequency drawing.


Figure 4. The use of frequency sharing for a frequency of 50 mHz.

auxiliary consumption used to demonstrate frequency sharing. The mission profile is given in Figure 1, and the filtering frequency is 50 mHz.

Figure 5 shows the changes in voltage for stored energy and fuel cells throughout the mission for the sizing proposed in Table 1. Using an ideal model, the state of charge of the stored energy and the limitation voltage of the fuel cell are within their limitations.
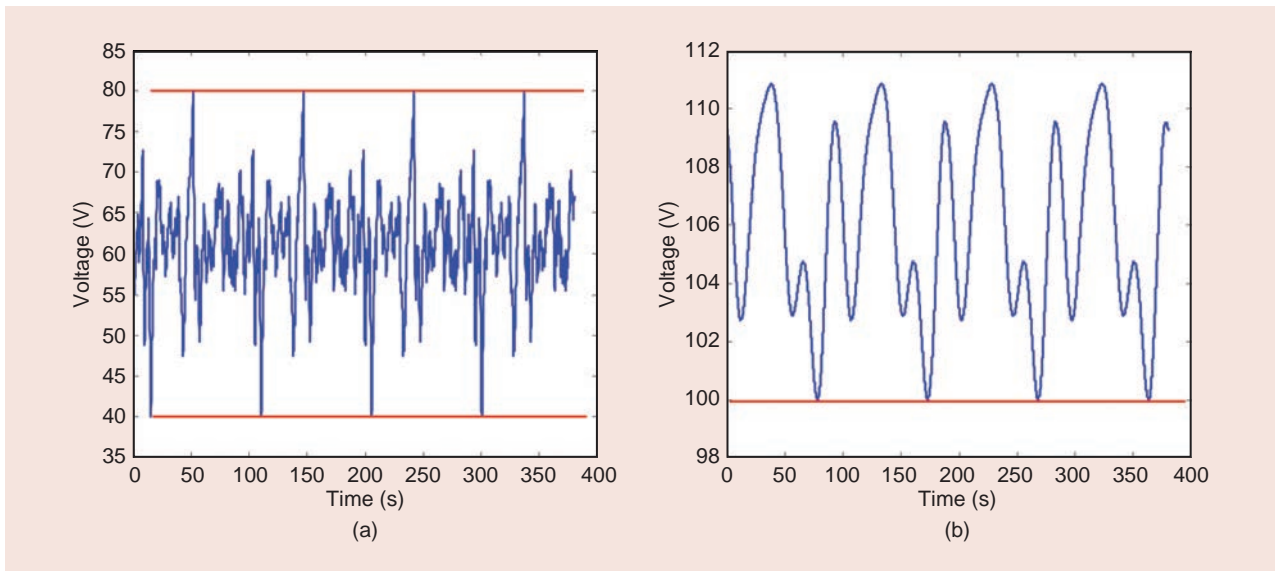
Figure 5. The voltages in (a) a storage device and (b) a fuel cell throughout the mission for the sizing displayed in Table 1.
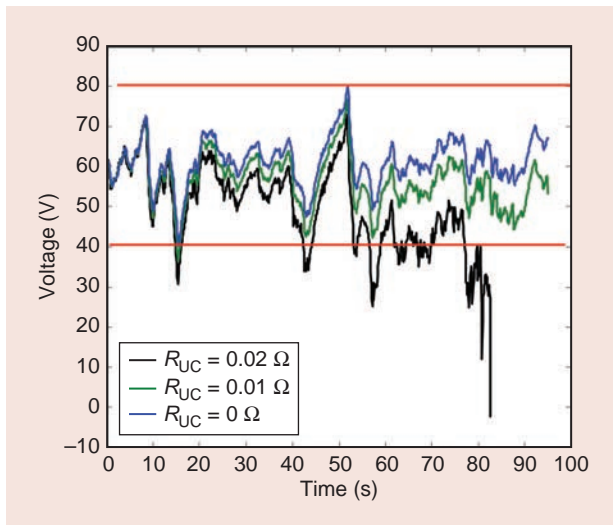
Figure 6. The ultracapacitor (UC) voltage evolution, taking into account losses due to internal resistances.
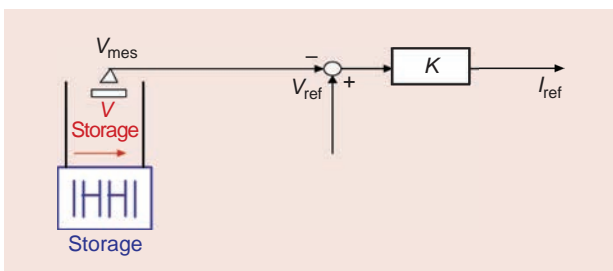
Figure 7. A control loop for the state of charge of the stored energy.

Impact of System Losses

Now, let us consider some losses in the system, in particular in the stored energy elements (the internal resistance of the ultracapacitors), as shown in Figure 6. An observation can be made that the state of charge of the stored energy is no longer within its limitations and that it moves toward a total discharge. In this case, the application quickly becomes no longer able to operate because all of the energy lost in stored energy losses is never compensated.

The solution put forward to maintain the state of charge of the stored energy is to add a proportional control loop coupled with a low-pass filter on the ultracapacitor voltage, as shown in Figure 7. The difficulty in choosing this corrector lies in choosing the proportional gain value K. With a gain K that is too low, the corrector will not be able to maintain the stored energy at a state of charge stable enough to be within its limitations. With a gain K that is too high, the stored energy voltage undulates at the frequency of the low-pass filter placed at the ultracapacitor voltage measurement point. Without this low-pass filter, high-frequency variations in the ultracapacitor voltage are carried onto the current provided by the fuel cell, which we aim to avoid. In addition, complying with the voltage limitations chosen for the stored energy is strongly linked to its reference voltage. Additionally, this loop must be included in the control of the system converter that is current controlled (with ultracapacitors first and fuel cells second) is because the converter that controls the bus voltage no longer has any degrees of freedom (DoF) to perform an additional function, in which case the bus voltage would be degraded.

Figure 8 shows various choices for the V_{ref} and K parameters of the control loop for the state of charge of the stored energy and the importance of the choice of these values for system stability. With a stored energy reference voltage that is too low, its mean state of charge cannot fulfill the entire mission. With a reference voltage for the stored energy that is too high, there is a risk of exceeding the maximum ultracapacitor voltage values. The choice of these values can help reduce (or increase, if poorly chosen)
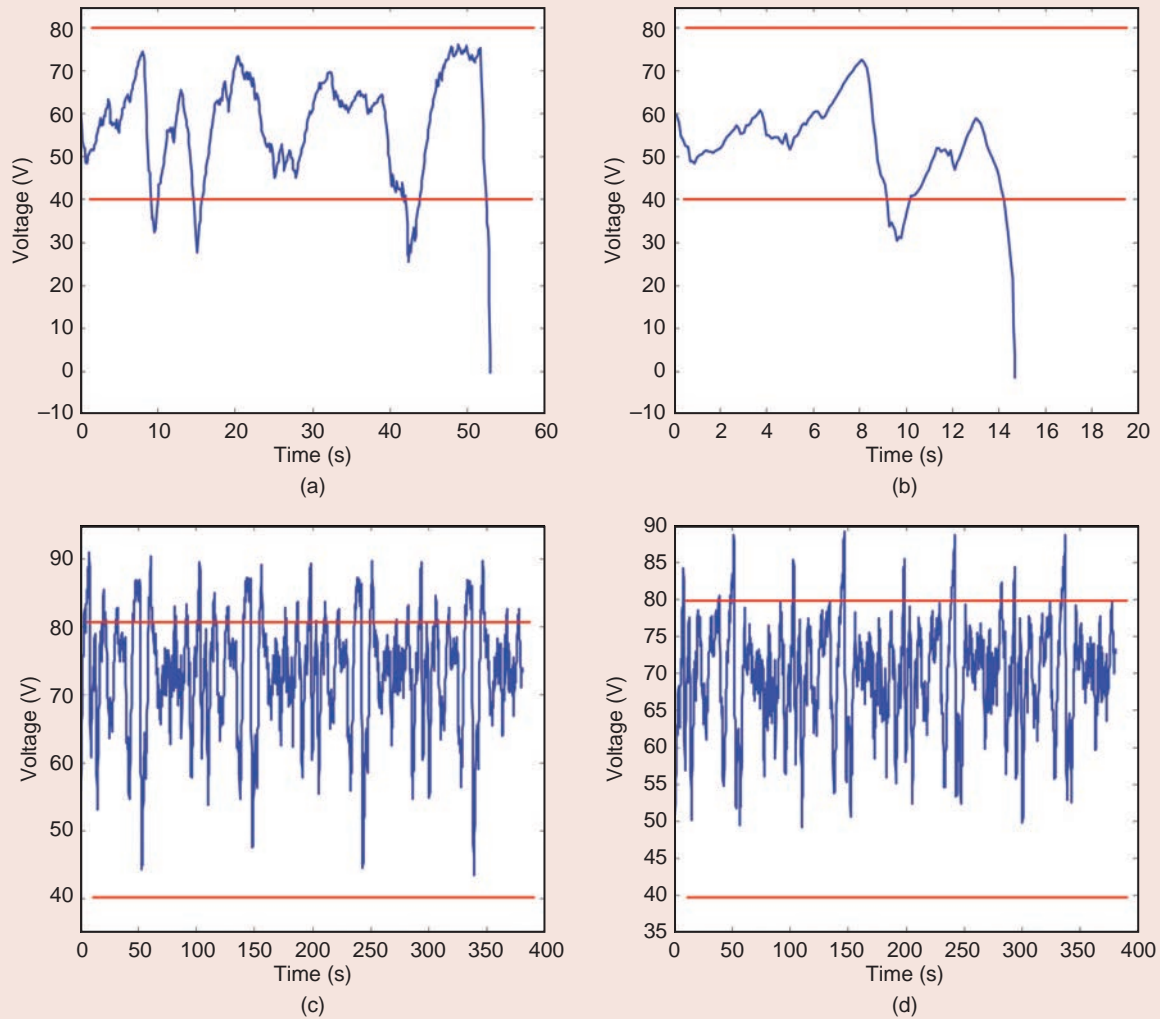
Figure 8. Some choices of parameters for the state-of-charge control loop: (a) gain = 5, V_{ref} = 60; (b) gain = 1.5, V_{ref} = 60; (c) gain = 5, V_{ref} = 72; (d) gain = 1.5, V_{ref} = 72.

the size of the stored energy system. Subsequently, the system sizing algorithm chooses these values.

In the prior discussed example (see Table 1), resizing the stored energy and its control loop using an iterative process from the optimization algorithm gives rise to the results in Table 2. Taking into account the stored energy losses and adding a loop to maintain the state of charge leads to a stored energy resizing that is around 23% higher than for the system when considered with no losses. It is also used to determine the criteria (reference voltage, proportional gain, and initial minimum voltage of the stored energy) enabling the mission to be performed, complying with the limitations set for the state of charge of the stored energy and ensuring its optimal operation (see in Figure 9).

Final Simulation Results
Two versions of the PEM fuel cell were studied by Garcia-Arregui: an H_2/O_2 stack and an H_2/air stack. The weight

TABLE 2. The results of iterative resizing with compensation for losses.

V_{ref} (V)	Gain	C (F)	V_0 (V)
68	3	12.1	47.5

savings that can be achieved with an H_2/O_2 stack (higher specific power and no compressor) is consequently canceled out due to the weight of the O_2 to be carried (mainly the weight of the tanks). For the weight minimization criteria, the solution from the theoretical studies is therefore the H_2/air solution. During the simulations, we considered a rather pessimistic scenario in which we took into account auxiliary consumption (mainly compressor consumption) equal to 20% of the fuel cell production as well as the losses in the converters (losses in switches, inductors, and capacitors). The simulation result for this system sizing is given in Figure 10.

Fuel cell production was noted to be higher than the mean load power. This would have also been valid in nonhybrid cases, taking into account the converter losses and the auxiliary consumption. However, the fuel cell supplies few high-frequency components, which should enable its compressor to correctly control the air supply flow rate and not speed up its aging. Compared to the ideal case presented in Figure 4, apart from the mean value for the power produced by the fuel cell, which differs for the reasons given above, slightly larger fluctuations can be seen for the supplied power. These fluctuations are due to the stored energy charging loop, which itself is dependent on its capacitance.

Implementation of the Selected Energy Management

DC Bus Voltage Control Strategy

As the architecture has two static converters, there is a DoF for controlling the bus voltage because there are three components connected to the dc bus: the loads, the stored energy and its converter, and the fuel cell and its converter. Only one of these elements can manage the bus voltage. Clearly, the loads cannot do this. It is therefore possible to control the bus voltage via the fuel cell converter or the stored energy converter.

Both of these solutions are shown in Figure 11. In some cases, it is of particular interest to assign the bus voltage management to the stored energy. This is true, e.g., when the fuel cell is replaced by a RAT, as maximum power

The high-frequency power components required by the application must be supplied by the ultracapacitors and the low-frequency components by the fuel cell.

point tracking can be associated with it (Rafal 2010, Langlois 2006). However, there currently seems to be minimal industry interest in a fuel-cell-based solution.

Regardless of the choice of dc bus control, frequency sharing must be performed as shown in Figure 3, i.e., the high-frequency power components required by the application must be supplied by the ultracapacitors and the low-frequency components by the fuel cell. This is achieved by a filter applied to the measured load current (Figure 11). The difference between both possible bus control strategies is that, when it is the fuel cell that commands the dc bus voltage [i.e., strategy one, Figure 11(a)], the converter associated with the stored energy must be more dynamically effective than the converter associated with the fuel cell. If it is less effective, the fuel cell will also inevitably supply the high-frequency components to control the bus. For strategy two [Figure 11(b)], the fuel cell will supply the low-frequency components only in the event its converter directly receives this instruction.

Dynamic Compensation of Losses

As explained in the "Impact of System Losses" section, losses in the converters and stored energy have a slow effect (low frequencies) on the state of charge of the stored energy and, therefore, on the system sizing. Ultimately, the fuel cell will have to supply power for these losses to maintain the state of charge for the stored energy.

However, for the strategy shown in Figure 11(a), these losses by the stored energy will consequently have only a
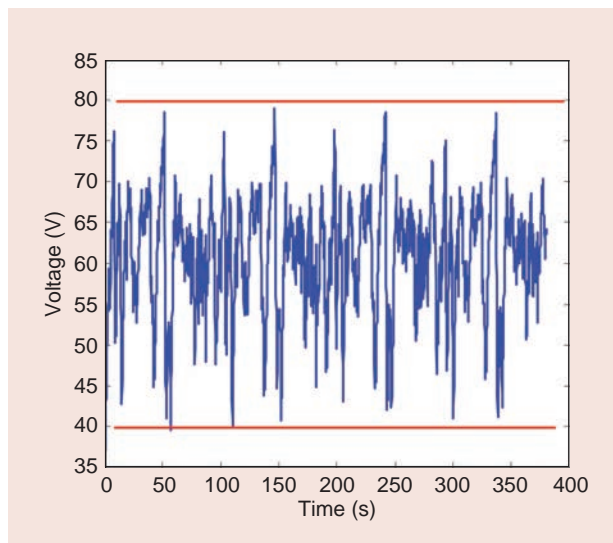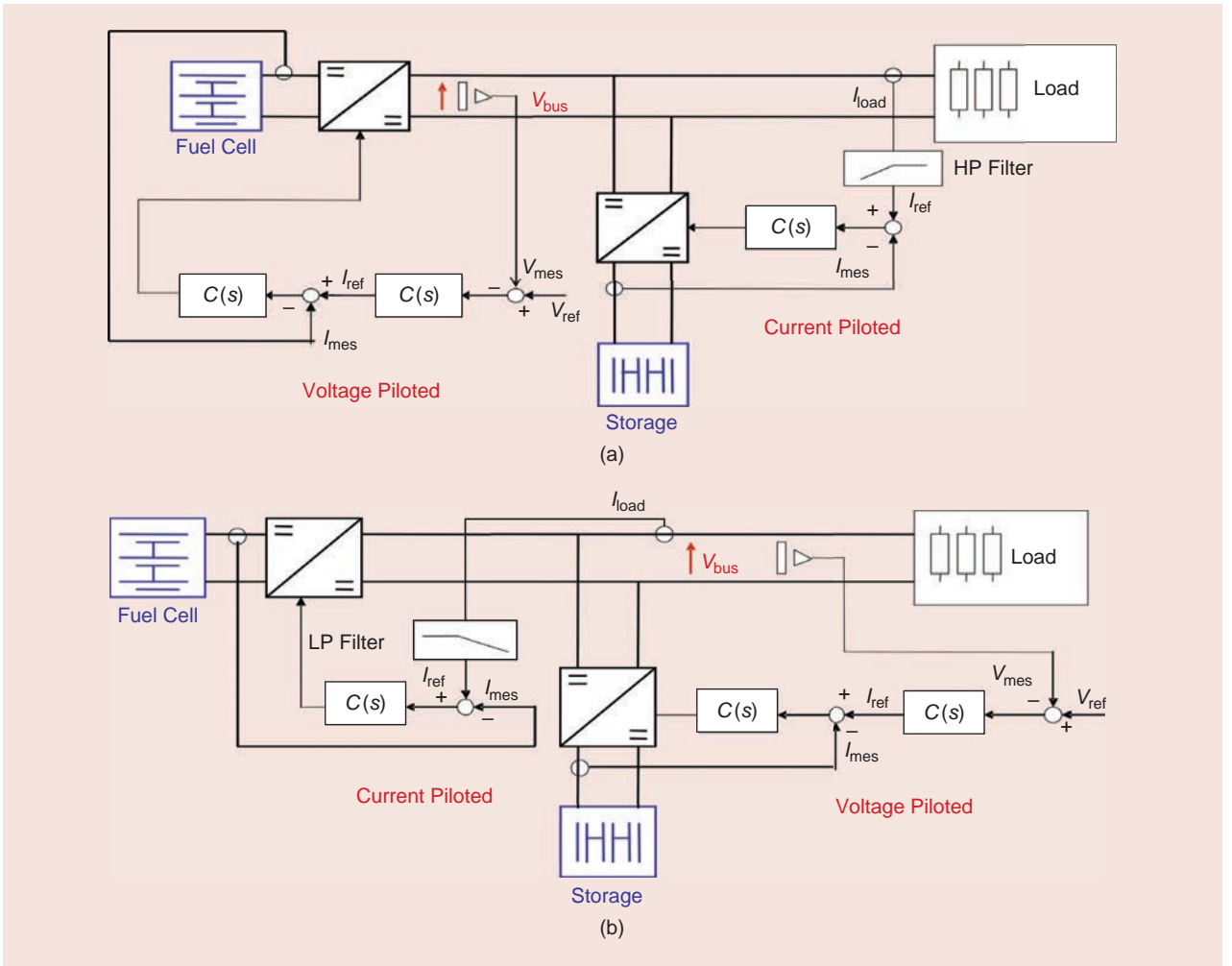

Figure 9. The change in stored energy voltage in resizing for the case in question (Table 1).
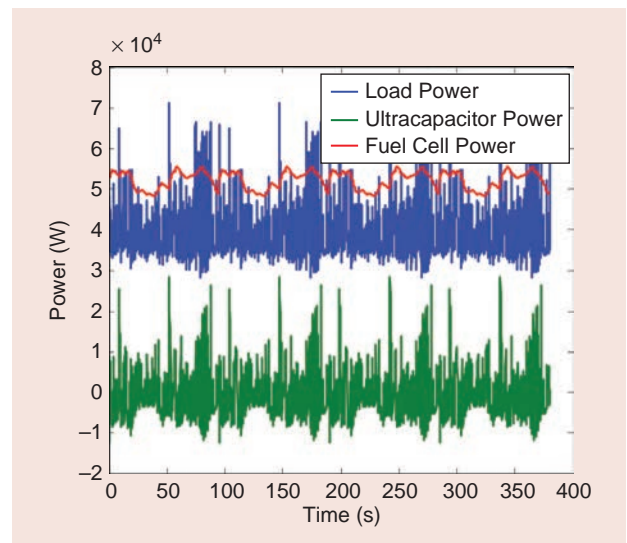
Figure 10. The power sharing obtained via simulation for the weight- and consumption-optimized system.

Figure 11. The DoF offered by the chosen architecture: (a) the bus managed by the fuel cell (strategy one); (b) the bus managed by the stored energy (strategy two). HP: high pass; LP: low pass.

partial supply of the high-frequency part of the load current, and this noncompensated part will therefore be found in the fuel cell current. Given the nature of the stored energy converter [dc–dc, bidirectional in current, working as a booster in the stored energy to bus direction (Rafal 2010)], it enables the current in the stored energy or the bus voltage to be controlled. In this case, we would like to control the converter output current, i.e., on the bus side, as the converter's instruction is to supply the high frequencies of the load current so that the fuel cell does not have to supply this part. As this current management method is not permitted because of the nature of the converter and we were not able to control this in our experimental system, a way of managing the current on the bus side would be to apply the voltage ratio to the reference current of the stored energy. This transposition requires a yield per unit from the converter. In practice, with no specific action, the final current at the bus will be lower than the current required. To be able to control the bus current via this converter, the chosen method is to add a converter loss compensation loop. The current was therefore managed as

$$I_{\text{Converter}}^{\text{HVdc}} \cong \frac{I_{\text{stor}} \cdot V_{\text{stor}} + P_{\text{L+Diodes+IGBT}}}{V_{\text{HVdc}}}, \qquad (2)$$

where $I_{\text{Converter}}^{\text{HVdc}}$ is the output current of the converter and I_{stor} is the input current to be managed. The equation includes converter losses. However, it is difficult to ascertain them in real time. We chose to compensate for them via a theoretical estimation. This is because the converter losses are mainly composed of losses in the switches (3) and (4)—here, the insulated-gate bipolar transistor (IGBT) and diode—in addition to losses in the passive elements (5):

$$P_{\text{IGBT}}(V, I) = P_{\text{cond}_{\text{IGBT}}} + P_{\text{comm}_{\text{IGBT}}}$$
$$= (V_{\text{CE}_0} \cdot \bar{I}_r + R_r \cdot I_{\text{eff}_r}^2 + (E_{\text{ON}}(V, I) + E_{\text{OFF}}(V, I)) \cdot f_{\text{dec}}) \quad (3)$$

$$P_{\text{Diode}}(V, I) = P_{\text{cond}_{\text{Diode}}} + P_{\text{comm}_{\text{Diode}}}$$
$$= (V_{\text{D}_0} \cdot \bar{I}_d + R_d \cdot I_{\text{eff}_d}^2) + (E_{\text{REC}}(V, I) \cdot f_{\text{dec}}) \quad (4)$$

$$P_L(I) = R_L \cdot I_L^2. \qquad (5)$$

Therefore, in requiring the stored energy to supply the high-frequency parts of the load power and the losses

calculated for its converter, full compensation for the load power high frequencies is close to being achieved. The mean value for these losses does not affect the control loop for the state of charge of the stored energy, as the losses are considered to be an additional load and go through the high-pass filter for the frequency sharing in Figure 11(a). The disadvantage of this method is that, if the estimation of these losses is incorrect or if they change over time (through component wear and tear), compensation no longer functions. The ideal solution would be a bidirectional dc–dc current converter for which we manage the current on the high-voltage side.

There is a similar situation for the strategy shown in [Figure 11(b)] because the converter associated with the fuel cell is a dc–dc unidirectional current boost converter (in the fuel cell to bus direction). It enables the management of the fuel cell current or the bus voltage. Here, we want to manage the current sent to the bus. As for the previous case, the losses are compensated by a theoretical estimation and considered to be an additional load. They therefore go through the low-pass filter for frequency sharing and are compensated using a mean value. The compensation for these losses has less of an effect on the hybridization performance as they have a low-frequency effect, which would be compensated for by the control loop for the state of charge of the stored energy.

Problem Starting the Frequency Sharing

Effective filtering for the fuel cell requires a low cutoff frequency for the frequency-sharing filter (here, 10 mHz). This means a long starting time for the filter. Used as is, the filter rise corresponds to the rise in the fuel cell current, i.e., during that whole time, the stored energy provides the power required for the loads. As the stored

> *The use of the emulator is less restrictive than using a fuel cell in terms of the cost of gas and the risk of damage.*

energy cannot fulfill this mission for long, it becomes fully discharged when the fuel cell reaches the mean current required by the frequency-sharing filter. Meanwhile, the bus voltage is no longer controlled as the stored energy is discharged and the mission is not fulfilled. At startup, there is an issue initializing this filter. Let us suppose that we are not aware of the steady state; we, therefore, cannot initialize the filter at its value in the steady state or at the value of the current at the startup time (in which case, we would risk starting on a peak). To compensate for these difficulties, we suggest successively switching to slower and slower filters to arrive at the final desired filter. Therefore, the chosen solution (shown in Figure 12) proposes starting with a fast filter (for which the cutoff frequency depends on the dynamics acceptable by the fuel cell and its fluidic regulations), while other slower filters start at the same time. Given the order of two and the damping factor ($\sqrt{2}/2$) of the filters, they naturally have a slight exceedance, which means that their values will inevitably coincide for a limited profile. This will enable switching to the lower-frequency filter with no value jumping. To prevent a return from a low-frequency filter to a higher-frequency filter, switching should be irreversible.

Small-Scale Experimental Validation

Description of the Experiment Performed

The experimental validation shown in Figure 13 takes place in two stages. The first is an experiment with the fuel cell replaced by an emulator, and the second is with an actual fuel cell. These trials will be used, among other things, to assess the relevance of an experiment employing an emulator and will guide the choice for full-scale validation. In addition, the use of the emulator is less restrictive than using a fuel cell in terms of the cost of gas and the risk of damage. It is used to adjust and validate all the control loops and push the strategies to their limits, with minimal risks for the equipment.

For the fuel cell, we have a stack of 50 cells measuring 130 cm^2, with H_2/O_2 operation, provided by AREVA Energy Storage Inc. [Figure 14(a)]. For the stored energy, we are equipped with 16-V, 58-F ultracapacitors (Maxwell Technologies' BMOD0058 E016). They will be connected in series, in a sufficient number to adapt to the level of the reference voltage for the stored energy [Figure 14(b)].

The load profile will be to scale based on the bench elements, i.e., 4 kW mean power and 8 kW peak power. Given the unique elements of the bench, the experiment could not take place in the exact sizing conditions resulting from the optimization.
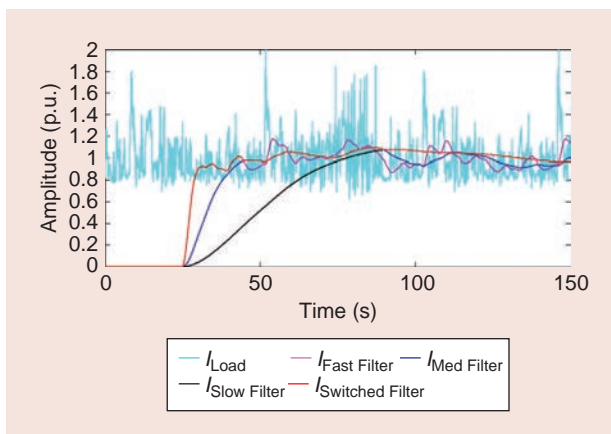
Figure 12. An example of filter switching. p.u.: per unit.

Emulation of a Fuel Cell

The fuel cell emulator consists of a programmable voltage source, with its output voltage adjusted to suit the current output so as to correspond to the almost static curve of a fuel cell. Its transfer function (taken from Fontes et al. 2007 and Rallieres 2011) is given by

$$V_{fc} = N.\left(E^0 + \frac{R.T}{n.F}.\ln\left(P_{H_2}.P_{O_2}^{1/2}\right) - \frac{R.T}{\alpha.n.F}.\ln\left(\frac{j+j_n}{j_0}\right) - R_{eq}.j\right) \quad (6)$$

where N is the number of cells in the stack, E^0 the standard nominal voltage of the H_2/O_2 redox pair, R the perfect gas constant, T the fuel cell temperature, n the number of electrons involved in the reaction, F Faraday's constant, and P_{H_2} and P_{O_2} the respective partial pressures of H_2 and O_2.

In addition, α (the transfer coefficient), j_n (the crossover equivalent current density), j_0 (the exchange current density), and R_{eq} (the membrane and diffusion equivalent surface resistance) are parameters taken per fitting on the actual almost static curve of an AREVA Energy Storage elementary cell, where $j = I/S$ is the current density going through our emulated fuel cell.

The experiment was conducted with a 1:10 ratio for the power with respect to the simulation results (Garcia-Arregui 2007). In addition, it was performed on a high-voltage dc half bus (i.e., +270 Vdc/0 Vdc instead of +270 Vdc/0 Vdc/−270 Vdc), which, in the end, is a 1:5 ratio for the power involved for this half bus.

Figure 15 shows power sharing via frequency filtering operated with the fuel cell emulator described previously.

We can see actual filtering of the load power by the stored energy. For both of these cases, we can see a certain thick area for the power supplied by the fuel cell. This thick area is due to our fuel cell emulator because the voltage source used for the emulator takes its power from the French network (230 Vac/400 Vac, 50 Hz) to supply its power. It is composed of a three-phase rectifier, then a dc–dc converter, which unfortunately allows some of the fundamental harmonic of the rectified network through (six times the network frequency, i.e., 300 Hz). As acquisition is performed with a step of 1 ms, these undulations appear.

However, for strategy one [Figure 15(a)], the high-frequency undulations are even more present. As expressed in the "dc Bus Voltage Control Strategy" section, this is due to a fuel cell converter bandwidth that is higher than the bandwidth of the stored energy converter, as well as an estimation of the dynamic losses for this converter that is not accurate, as it is based on theoretical calculations. The frequency band for these phenomena is found at the fuel cell current, as the frequencies are too high to be managed by the stored energy converter. This frequency band is in addition to the 300-Hz undulation supplied by the fuel cell emulator.

System Stability

Using the emulator tests the system to its limits and notably tests the stored energy stability. To test this power management stability, we considered two situations that are theoretically the worst cases that could cause the system difficulties:
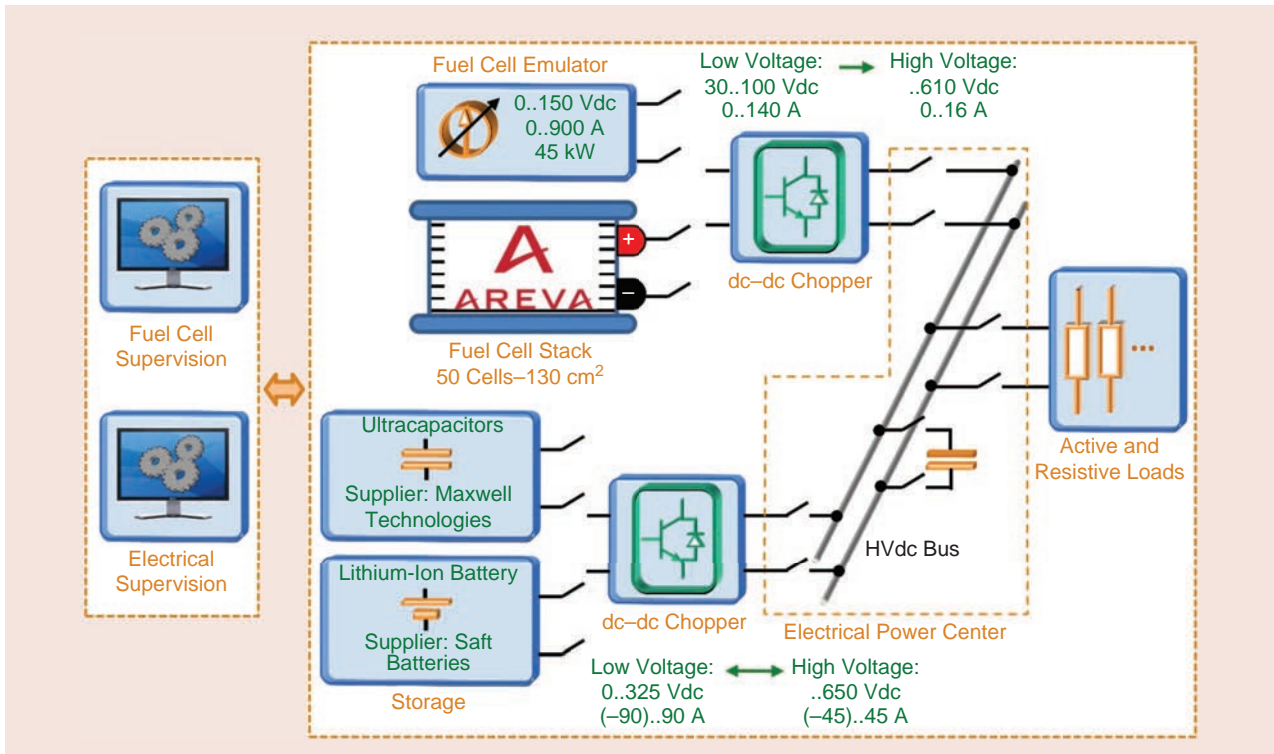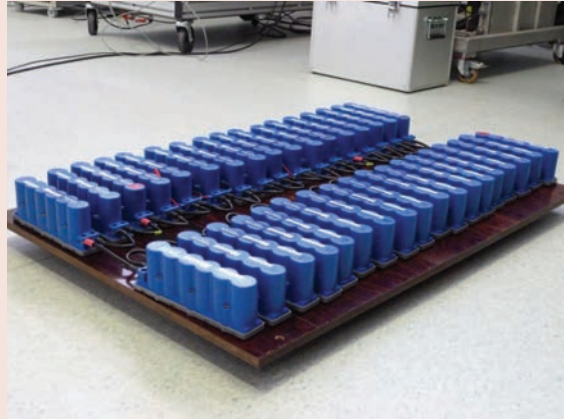

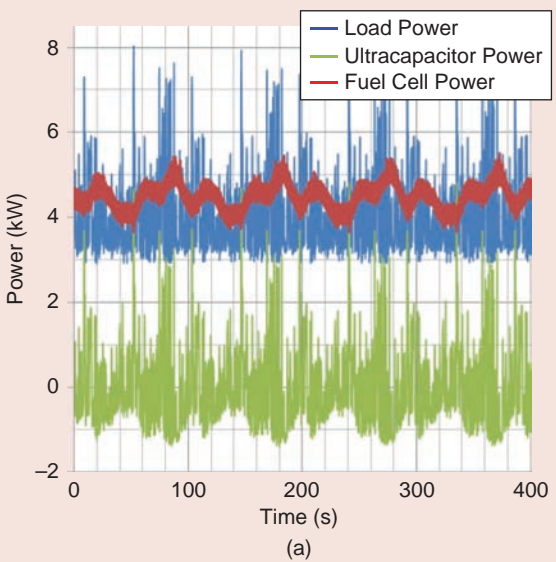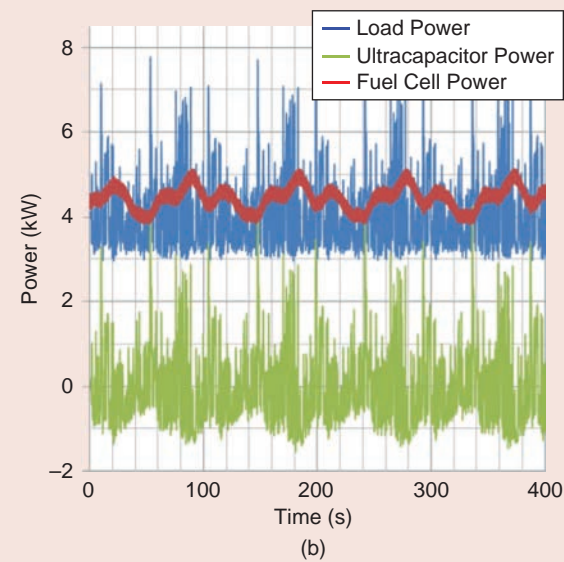**Figure 13.** A diagram and structure of the test bench for the experiment.

Figure 14. Photos of the test bench elements: (a) the fuel cell test bench; (b) the ultracapacitors; (c) the electrical prototypes; (d) and the monitoring room.
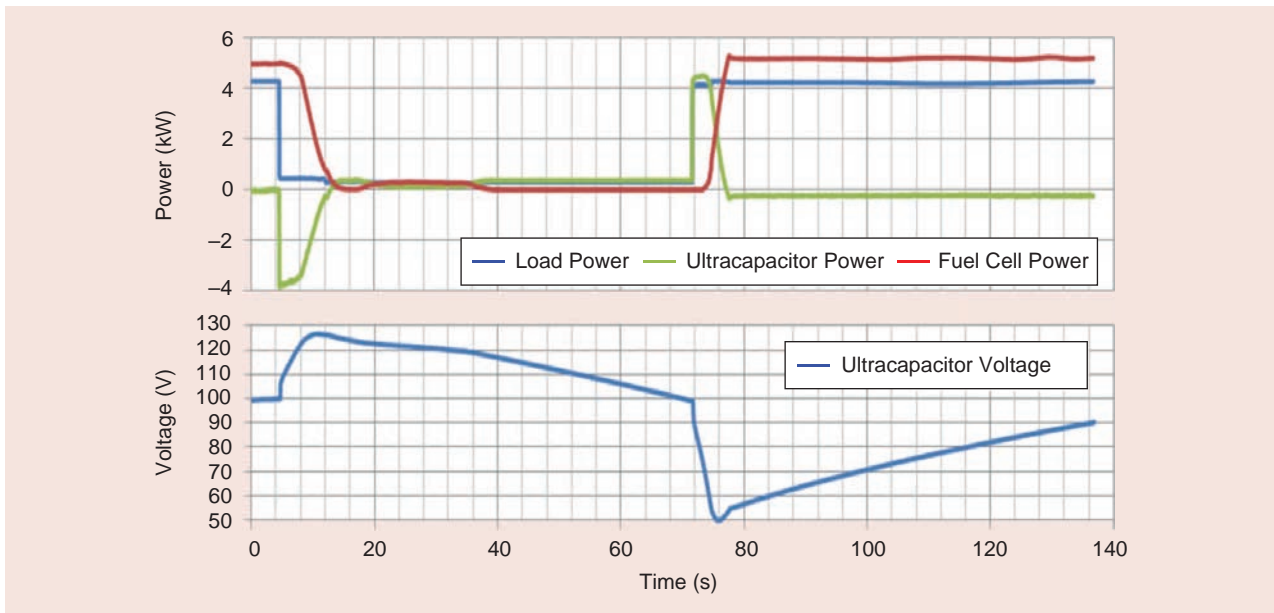

Figure 15. Power sharing achieved via an experiment with a fuel cell emulator: (a) a bus managed by the fuel cell (strategy one); (b) a bus managed by the stored energy (strategy two).
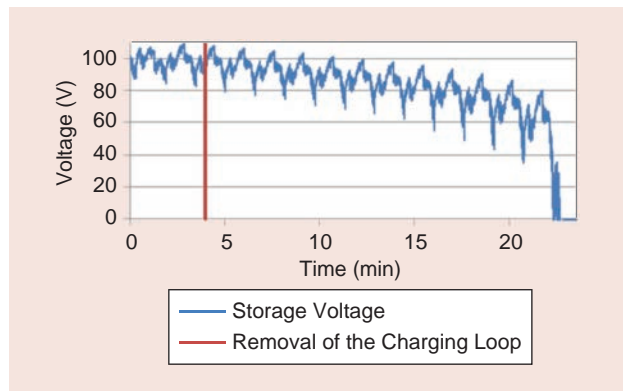
Figure 16. A stored energy charging loop enters into difficulty.

▶ Case 1: The load disconnects (step of nominal one to zero); all of the current supplied by the fuel cell is therefore absorbed by the ultracapacitors; they charge but must above all not exceed their maximum voltage.

▶ Case 2: The load reconnects (step of zero to nominal one); the ultracapacitors empty to supply the power required for the load, but they must not discharge too substantially so the system can continue to operate.

This is shown in Figure 16, where we guarantee that the state of charge for the stored energy does not endanger the system when faced with these two situations. The high and low limits for the stored energy are 150 V and 0 V.

Figure 17 shows the purpose of the stored energy charging loop described in the "Impact of System Losses" section. Indeed, when this loop is not present, the stored energy starts to completely discharge, and the more its state of charge decreases, the higher the requested currents, which makes the voltage decrease even further at its limitations.

The issue of starting for hybridization mentioned in the "Problem Starting the Frequency Sharing" section must be experimentally validated to check the stability of the filter switching with the stored energy charging loop. This is because hybridization, when starting, is launched with all of the power consumed by the loads supplied by the stored energy; its state of charge decreases very quickly, and its control loop will tend to increase the power supplied by the fuel cell to recharge it. Figure 18 shows this startup for a test with an emulator. The fuel cell quickly reaches its nominal power, and we can easily distinguish between the moments where the frequency-sharing filter switches thanks to the
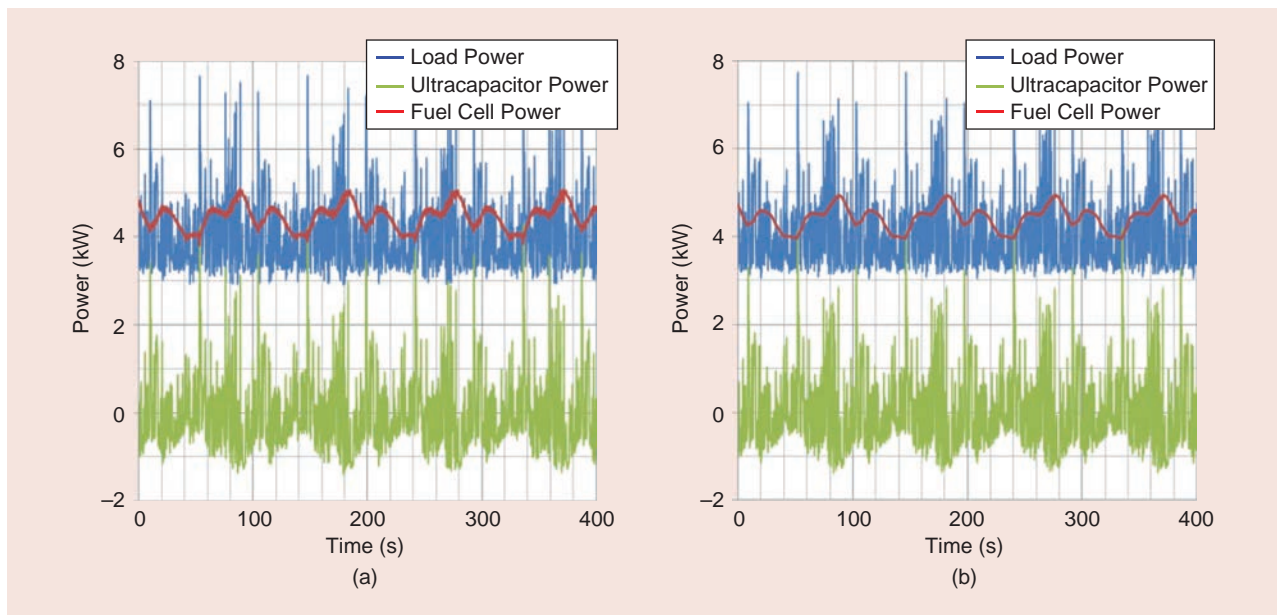

Figure 17. A stored energy charging loop suppression.
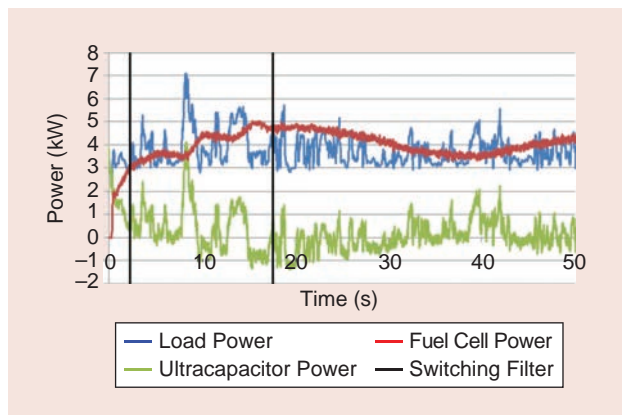
Figure 18. Hybridization startup with an emulator.

harmonics present on the power supplied by the fuel cell. The experiment on the fuel cell power increase is in line with the theoretical switching of the filters shown in Figure 12.

Figure 19. Power sharing achieved via an experiment with an actual fuel cell: (a) a bus managed by the fuel cell (strategy one); (b) a bus managed by the stored energy (strategy two).

Tests with an Actual Fuel Cell

The tests in Figure 15 were repeated with the real fuel cell stack, the characteristics of which are given in the "Description of the Experiment Performed" section.

Figure 19 shows the hybridization tests with the fuel cell stack for both strategies put forward in this article. The same phenomena as in Figure 15 can be seen, with one less high-frequency undulation because a significant part of the high-frequency part present at the power supplied by the fuel cell emulator was due to the three-phase electrical network. As the fuel cell is a dc source, these undulations no longer appear. However, even more harmonics provided by the fuel cell are found in strategy one for the same reasons as in the "Emulation of a Fuel Cell" section, i.e., a stored energy converter that is less dynamically effective than the fuel cell converter.

Conclusions

Going from simulation to experiment confirmed the theoretical results but also revealed phenomena that were not apparent during the simulations (e.g., interference between the converters, voltage rise of the elements, connections between them, immunity to noise, resonance, and so forth). In addition, while Figures 10 and 19 are relatively similar, we can see that the mean current provided by the fuel cell during the simulations (Figure 5) is higher than that observed in the experiment. This is due to the ultracapacitor technology, which had developed in the meantime (the internal resistance is now lower than during the theoretical study), but is also due to the scale factor, which considered the losses to be greater in the more powerful converters. However, the emulation showed very satisfactory results with respect to the experiment with an actual fuel cell, confirming all of the

potential offered by fuel cell emulation (e.g., to go toward full scale in terms of power). This work was continued by replacing the ultracapacitors with a battery for different aviation specifications (Jaafar et al. 2014).

For Further Reading

J. A. Weimer, "Electrical power technology for the more electric aircraft," in *Proc. 12th AIAA/IEEE Digital Avionics Syst. Conf.*, Oct. 1993, pp. 445–450.

X. Roboam, B. Sareni, and A. D. Andrade, "More electricity in the air: Toward optimized electrical networks embedded in more-electrical aircraft," *IEEE Ind. Electron. Mag.*, vol. 6, no. 4, pp. 6–17, 2012.

J. A. Rosero, J. A. Ortega, E. Aldabas, and L. Romeral, "Moving toward a more electric aircraft," *IEEE Aerosp. Electron. Syst. Mag.*, vol. 22, no. 3, pp. 3–9, Mar. 2007.

I. S. Mehdi and E. J. Woods, "Electrical power systems for high mach vehicles," in *Proc. IEEE Energy Conversion Engineering Conf.*, Washington, DC, 1989, pp. 625–630.

P. Bolognesi, F. Papini, and L. Taponecco, "Hybrid-excitation dc machines as highly reliable generators for ram air turbines," in *Proc. IEEE Industrial Electronics Society Conf.*, Porto, Portugal, 2009, pp. 2569–2574.

D. Van Den Bossche, "More electric control surface actuation: A standard for the next generation of transport aircraft," in *Proc. 10th European Power Electron. and Applicat. Conf.*, Toulouse, France, 2003, pp. 1–6.

M. Garcia-Arregui. (2007). Theoretical study of a power generation unit based on the hybridization of a fuel cell stack and ultracapacitors. Ph.D. dissertation, Institut. Nat. Polytech.,

Toulouse, France. [Online]. Available: http://ethesis.inp-toulouse.fr/archive/00000521/

A. Wörner, "Fuel cells and hydrogen for airborne applications," in *Proc. NWV 7th Nat. Hydrogen and Fuel Cell Conf.*, Arnhem, Germany, Dec. 2009.

S. N. Motapon, L. Dessaint, and K. Al-Haddad, "A comparative study of energy management schemes for a fuel-cell hybrid emergency power system of more-electric aircraft," *IEEE Trans. Ind. Electron.*, vol. 61, no. 3, pp. 1320–1334, 2014.

S. N. Motapon, L. Dessaint, and K. Al-Haddad, "A robust-consumption-minimization-based energy management strategy for a fuel cell hybrid emergency power system of more electric aircraft," *IEEE Trans. Ind. Electron.*, vol. 61, no. 11, pp. 6148–6156, 2014.

M. C. Pera, D. Hissel, H. Gualous, and C. Turpin, Eds., *Electrochemical Components*. Hoboken, NJ: Wiley, 2013.

B. Lenz and T. Aicher, "Catalytic autothermal reforming of jet fuel," *J. Power Sources*, vol. 149, pp. 44–52, Sept. 2005.

A. F. Ibarreta and C.-J. Sung, "Optimization of Jet-A fuel reforming for aerospace applications," *Int. J. Hydrogen Energy*, vol. 31, no. 8, pp. 1066–1078, 2006.

S. Curtin, "Fuel cells flying high," *Int. Airport Rev.*, no. 4, pp. 36–39, 2010.

A. Eid, H. El-Kishky, M. Abdel-Salam, and T. El-Mohandes, "Modeling and characterization of an aircraft electric power system with a fuel cell-equipped APU connected at HVDC bus," in *Proc. 2010 IEEE Power Modulator and High Voltage Conf. (IPMHVC)*, Atlanta, GA, pp. 639–642.

K. Rajashekara, J. Grieve, and D. Daggett, "Hybrid fuel cell power in aircraft," *IEEE Ind. Applicat. Mag.*, vol. 14, no. 4, pp. 54–60, 2008.

C. Turpin, S. Astier, X. Roboam, B. Sareni, and H. Piquet, *Systemic Design Methodologies for Electrical Energy Systems*. Hoboken, NJ: Wiley, 2012.

X. Roboam, O. Langlois, H. Piquet, B. Morin, and C. Turpin, "Hybrid power generation system for aircraft electrical emergency network," *IEEE IET Trans. Elect. Syst. Transp.*, vol. 1, no. 4, pp. 148–155, 2011.

K. Rafal, B. Morin, X. Roboam, E. Bru, C. Turpin, and H. Piquet, "Hybridization of an aircraft emergency electrical network: Experimentation and benefits validation," in *Proc. IEEE Vehicle Power and Propulsion Conf. (VPPC)*, Lille, France, 2010, pp. 1–6.

Z. Jiang and R.A. Dougal, "A hybrid fuel cell power supply with rapid dynamic response and high peak-power capacity," in *Proc. 21st IEEE Applied Power Electronics Conf. and Exposition*, Dallas, TX, 2006, pp. 1250–1255.

J. S. Martínez, D. Hissel, M. C. Péra, and M. Amiet, "Practical control structure and energy management of a testbed hybrid electric vehicle," *IEEE Trans. Veh. Technol.*, vol. 60, no. 9, 2011.

N. Bizon, M. Stork, and M. Oproescu, "Fuel cell hybrid power source for pulsed current loads," in *Proc. IEEE 2012 Int. Conf. Applied Electronics,* 2012, pp. 25–28.

Y. Zhan, Y. Guo, J.-G. Zhu, and H. Wang, "Power converters and controllers for UPS applications with backup PEM fuel cell," in *Proc. IEEE Industry Applications Society Annu. Meeting*, 2008, pp. 1–8.

B. Morin, D. Van Laethem, C. Turpin, O. Rallières, S. Astier, A. Jaafar, O. Verdu, M. Plantevin, and V. Chaudron, "Direct hybridization fuel cell–ultracapacitors," *Fuel Cells*, vol. 14, no. 3, pp. 500–507, 2014.

P. Ravel, "Electrical distribution of high power: Impacts, technologies," in *Proc. More Electric Aircraft Forum*, Barcelona, Spain, Sept. 2009, pp. 8–11.

S. J. Moura, J. B. Siegel, D. J. Siegel, H. K. Fathy, and A. G. Stefanopoulou, "Education on vehicle electrification: Battery systems, fuel cells, and hydrogen," in *Proc. IEEE Vehicle Power and Propulsion (VPPC)*, Lille, France, 2010, pp. 1–6.

P. Flynn, *Meeting the Energy Needs of Future Warriors*. Washington, D.C.: National Academies Press, 2004.

O. Langlois (2006). Conception d'un réseau de secours électrique pour l'aéronautique. Ph.D. dissertation, Institut. Nat. Polytech., Toulouse, France. [Online]. Available: http://ethesis.inp-toulouse.fr/archive/00000243/

Maxwell Technologies Inc. (2017). Maxwell. [Online]. Available: www.maxwell.com

L. Schindele, M. Braun, and H. Spath, "The influence of power electronic dynamics on PEM fuel cell system," in *Proc. IEEE EPE Conf. Power Electronics and Applications,* Dresden, Germany, 2005, pp. 1–9.

P. Thounthong and P. Sethakul, "Analysis of a fuel starvation phenomenon of a PEM fuel cell," in *Proc. IEEE Power Conversion Conf. (PCC)*, Nagoya, Japan, 2007, pp. 731–738.

P. Chapoulie and S. Astier, "Modelling of an electric vehicle including ultracapacitors with SABER," in *Proc. Int. Electric Vehicle Symp. Exposition*, Brussels, Belgium, Sept. 1998, pp. 1–3.

AREVA Energy Storage Inc. AREVA. [Online]. Available: www.areva.com

G. Fontes, C. Turpin, S. Astier, and T.A. Meynard, "Interactions between fuel cells and power converters: Influence of current harmonics on a fuel cell stack," *IEEE Trans. Power Electron.*, vol. 22, no. 2, pp. 670–678, 2007

O. Rallieres, "Modélisation et caractérisation de piles à combustible et électrolyseurs PEM," Ph.D. dissertation, Institut. Nat. Polytech., Toulouse, France, 2011.

N. Lapena-Rey, J. Mosquera, E. Bataller, F. Ortı, C. Dudfield, and A. Orsillo, "Environmentally friendly power sources for aerospace applications," *J. Power Sources*, vol. 181, no. 2, pp. 353–362, 2008.

A. Jaafar, C. Turpin, X. Roboam, E. Bru, and O. Rallières, "Energy management of a hybrid system based on a fuel cell and a battery," in *IEEE Int. Conf. Modeling and Simulation of Electric Machines, Converters and Systems (ElectrIMACS),* Valencia, Spain, 2014, pp. 1–6.

Biographies

Christophe Turpin (turpin@laplace.univ-tlse.fr) is with the Université de Toulouse, France.

Benoît Morin (benoit.morin@cea.fr) is with the French Atomic Energy and Alternative Energy Commission, the Research Institute on New Energy Technologies and Nanomaterials, Grenoble, France.

Eric Bru (bru@laplace.univ-tlse.fr) is with the Université de Toulouse, France.

Olivier Rallières (ralarieres@laplace.univ-tlse.fr) is with the Université de Toulouse, France.

Xavier Roboam (roboam@laplace.univ-tlse.fr) is with the Université de Toulouse, France.

Bruno Sareni (sareni@laplace.univ-tlse.fr) is with the Université de Toulouse, France.

Marcos Garcia Arregui (marcosgarcia.arregui@gmail.com) is with General Electric, Belfort, France.

Nicolas Roux (roux@laplace.univ-tlse.fr) is with the Université de Toulouse, France.